The Chemisorption of Pyridine on Plasma-Grown Aluminium Oxide: An Inelastic Electron Tunneling Spectral Study

N. M. D. BROWN, D. G. WALMSLEY, AND R. B. FLOYD

School of Physical Sciences, The New University of Ulster, Coleraine, Northern Ireland

From a detailed consideration of the inelastic electron tunneling (IET) spectra of pyridine-vapor-doped Al/Al oxide/Pb tunnel junctions, it is found that pyridine is adsorbed at both Lewis acid and Brønsted active sites present on the plasma-grown oxide surface. The data presented are compared with that of air-grown oxide, fluorided air-grown oxide, and with the known behavior of bulk aluminas.

INTRODUCTION

Since Jaklevic and Lambe (*1*) first obtained vibrational spectra of organic molecules adsorbed on barrier oxides by excitation with tunneling electrons, several spectroscopic applications of the inelastic electron tunneling (IET) method have been reported. These, and basics of the technique, have recently been reviewed (*2*). Moreover, it is now clear that inelastic electron tunneling spectroscopy (IETS) is capable of giving vibrational spectra of good quality over the 300- to 4000-cm^{-1} range even at very low surface coverages, ∼1/30 of a monolayer or less (*3*). As such, the IET method is clearly useful in the study of surface adsorbates. While the IET method is in principle applicable to a much wider range of adsorbents, almost all of the work published so far has, for a number of reasons, dealt with organic species adsorbed on a thin layer of aluminum oxide. This oxide is grown on the metal either by exposure to air or to oxygen. Though some evidence exists (*4*) that thick oxide films

prepared in this way at moderately high temperatures are γ-alumina in type, we believe thin films are more likely to be amorphous (*5*). The latter may have adsorption characteristics and possible catalytic behavior which differ from those of bulk alumina. It follows, therefore, that much of the IET work at present underway is directed to the question of how these films of aluminium oxide compare with bulk alumina.

We report here our IETS results on pyridine adsorbed at room temperature from vapor on to plasma-grown aluminium oxide as a gauge of the acidity (*6, 7*) of this type of surface. A comparison is made with available optical vibrational data of pyridine adsorbed on bulk aluminas and with the IETS study of pyridine adsorbed on to air-grown oxide recently reported by Hansma *et al.* (*8*).

A feature of the study of air- or plasma-grown oxides on aluminium is the ease with which a surface of reproducible chemical character can be prepared.

EXPERIMENTAL CONSIDERATIONS

(a) *Sample preparation.* Our usual procedure was followed in the present case. In this, three Al–aluminium oxide–Pb junctions are made simultaneously on a glass microscope slide which has been carefully cleaned. Aluminium is first evaporated from a multistranded tungsten filament to form a strip 60 mm long, 0.7 mm wide and ∼1000 Å thick. A thin oxide layer (∼20 Å) is then grown on this in a dc plasma established in an oxygen atmosphere at a pressure of 0.03 Torr with a plasma current of 5 mA maintained for 30–90 s. This oxide is then exposed at room temperature to the vapor of dry, redistilled pyridine (A.R. grade) by opening the evacuated (∼10⁻⁶ Torr) evaporator to a suitable reservoir of liquid. A quartz crystal located close to the slide is used in the conventional manner as an adsorption microbalance to monitor vapor deposition. Several trials showed that while pyridine was absorbed on a room-temperature adsorbent oxide nearly all of this was subsequently pumped off in the process of completing the junction. However, by cooling the surface to 200 K before evacuating the chamber and laying down the ∼7000-Å-thick top lead counter electrodes, a reproducible amount of pyridine was retained by the oxide. Filament and mask changes were carried out with the system under vacuum, the supporting slide remaining *in situ* during all stages of junction preparation. The Edwards E12E vacuum evaporator used is pumped by a diffusion pump charged with a very stable high-boiling oil, SANTOVAC 5; the backing line is fitted with a zeolite trap. After removal of the sample from the evaporator it is mounted on a Tufnol holder, leads are attached with indium solder, and the whole assembly is suspended from a stainless-steel tube in a standard double-glass helium cryostat which is pumped to 2 K. Acceptable doped tunnel junctions have resistances in the range of 20–200 ohms.

(b) *Signal detection.* The inelastic processes which correspond to the vibrational excitations of interest show up as very small changes in the gradient of the current-voltage characteristic of the tunnel junction under study. To locate the energies at which these changes occur, ac modulation techniques are used. The circuit at present in use has been described in detail (9) elsewhere. A 2.0-mV peak-to-peak 50-kHz signal is applied to the swept dc bias voltage across the tunnel junction in conjunction with a discriminant filter network which accepts the second harmonic (100 kHz) but rejects the fundamental prior to the Ortec Brookdeal 9501 lock-in amplifier used as detector. This mode of detection, via the second harmonic, gives the "absorption" lines which are observed as d^2V/dI^2 vs V, on an X–Y recorder. The dc bias, V, of the junction is swept by a motor driven potentiometer through $0 \rightarrow 500$ mV and displayed on the X-axis of the recorder with the second derivative as ordinate.

RESULTS AND DISCUSSION

The IET spectrum of a pyridine-doped junction is shown in Fig. 1 alongside that of an undoped Al–Al oxide–Pb junction. The latter shows only the usual ν(O–H) and ν(Al–O) modes, close to 3600 and 940
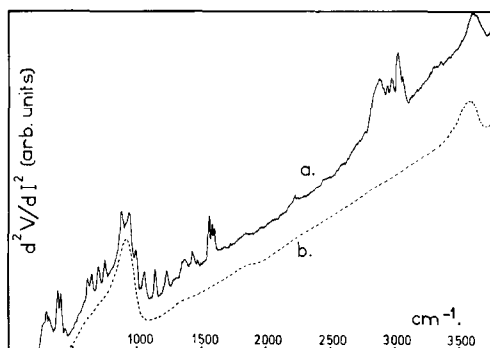

FIG. 1. IET spectrum (obtained at 2 K) (a) Pyridine adsorbed on plasma-grown aluminium oxide and (b) clean undoped Al–aluminium oxide–Pb tunnel junction.

TABLE 1

IET Spectral Data of Chemisorbed Pyridine on Plasma-Grown Aluminum Oxide and Related Vibrational Data

Symmetry[a]	IETS bands			Vibrational modes				
	Plasma-grown oxide[b] (cm⁻¹)	Air-grown oxide[c]		Pyridine[d] (cm⁻¹)	Pyridinium ion[d] (cm⁻¹)	Pyridine complexes[e] (cm⁻¹)	Pyridine on γ-Al₂O₃ Raman bands[f] (cm⁻¹)	Likely assignments[d]
		Fluoride[d] (cm⁻¹)	Heat-treated (cm⁻¹)					
		1637 w	—		1637	1625–1650		
	1613 (1.00) sh	1612 s	1605 sh		1610		1613[g]	ν(C–C)
a₁	1593 (1.25)	—	1583 s	1583		1597–1604	1594	ν(C–C)
b₂	1572 (1.75)	1573 s	1572 s	1572		1568–1575	1577[g]	ν(C–C)
b₂	1550 (0.50) sh	1547 w	—		1538			ν(C–C)
a₁	1482 (0.40)	1490 mw	1481 w	1482	1488	1478–1489		ν(C–C)
b₂	1446 (0.75)	1447 s	1433 s	1439		1440–1449		ν(C–C)
b₂	1386 (0.75)	1372 w	1372 w	1375	1383	1370–1400		ν(C–C)
a₁,b₂	—	—	—		1330			β(C–H) +
b₂	1245 (0.75)	1248 m	1258 br		1250	1235–1242		β(N–H)
a₁,b₂	1220 (0.25) sh	—	—	1218, 1218	1202	1215–1221	1222[g]	β(C–H)
b₂	1159 (1.00)	1165 ms	1153 m	1148	1170	1144–1168		β(C–H)
b₂	—	—	1112 m	1085	1050, 1050	1068–1082		β(C–H)
a₁	1068 (1.00)	1074 m	1064 m	1068	1050, 1050	1068–1082		β(C–H)
a₁	—	—	1025 w	1030	1026	1035–1042	1032, 1019[g]	ring
a₁	1003 (1.75)	1003 m	—	992	1009	1005–1016	999, 991	breathing
a₂	—	—	975 m	981	997			γ(C–H)
b₁	948 (1.00)	—	—	942		930–970		γ(C–H)
b₁	—	928 w	920 m	942		930–970		γ(C–H) +
b₁	—	—	—	—	895			γ(N–H)
a₂,b₁	887 (1.50)[h]	880[h]	860[h]	886, 886	806			γ(C–H)
	—	—	786 m					γ(C–H)
b₁	761 (1.10)	760 m	—	749	748	750– 769		γ(C–H)
b₁	—	—	740 m	749	748	750– 769		γ(C–H)
b₁	714 (1.00)	702 m	701 m	700		680– 713		γ(C–C)
b₁	—	—	—		675			γ(C–H)
b₂	655 (1.25)	650 ms	—	652	637	645– 650	653[g]	β(C–C)
a₁	625 (1.50)	—	615 m	605	608	622– 641		β(C–C)
	—	—	478 m					
	454 (0.50)	448 m	—					
b₁	418 (1.75)	—	—	405				γ(C–C)
a₂	393 (2.00)	390 s	404 s	374				γ(C–C)
	302 (0.45)	—	—					γ(C–C)
b₂	3074 (1.00) sh			3083	3090		3079	ν(C–H)
a₁	3044 (2.25)			3054, 3054	3050		3060[g]	ν(C–H)
a₁,b₂	2994 (1.50)			3036, 3036				ν(C–H)
	2964 (1.25)				3268			ν(C–H) +
	2897 (2.00) vbr							ν(N–H)

[a] C₂ᵥ symmetry assumed, see text and d.
[b] Our data, intensities scaled against 1159-cm⁻¹ band; sh, shoulder; vbr, very broad.
[c] From Hansma et al. (8); s, strong; m, medium; w, weak.
[d] Taken from Ref. (11) and references therein; β, in-plane bend; γ, out-of-plane.
[e] Taken from Ref. (12).
[f] Taken from the study of Hendra and co-workers (13).
[g] Retained and observed at very low surface coverages.
[h] Superimposed on background ν(Al–O) mode.

cm⁻¹, respectively. Bands due to surface bound molecular water expected (10) at ~3300 and ~1630 cm⁻¹ are absent. We note that a rigorously dry oxygen plasma fails to give satisfactory oxide films; the surface hydroxyl present arises therefore from traces of water in the oxygen supply used.

Table 1 lists the IET spectral data[1] along with the fundamentals of the pyridinium ion and pyridine itself (11), pyridine complexes (12), and the significant Raman bands of pyridine adsorbed on γ-alumina (13). For comparison with IET data of pyridine adsorbed on the differently treated thermally grown oxide of Hansma and co-workers (8) are also given.

Since the orientation dependence of the IET line intensities is still under active discussion (14) we have labeled the various bands under a C_{2v} regime with the assumption that this is retained at the surface of the oxide. The axes chosen are those recommended (15): The C_2 axis, which may or may not be aligned parallel to the direction of tunneling, is that through nitrogen and C-4; the yz-plane is the plane of the molecule with the x-axis perpendicular at the center of the pyridine ring. The resultant fundamentals are then distributed as

$$\Gamma = 10a_1(\text{ir}, R) + 3a_2(R) + 5b_1(\text{ir}, R) \\ + 9b_2(\text{ir}, R);$$

interchange of the x and y axes simply interchanges the b_1 and b_2 labels. The band intensities indicated are scaled arbitrarily against that of the line at 1159 cm^{-1} set to unity. Given that the symmetry assignments are applicable, then the out-of-plane (a_2, b_1) modes have an average intensity some 15% more than the in-plane (a_1, b_2) modes. A theoretical treatment of the corresponding ir band intensities is available for comparison (16). Linewidths are some three times greater than the calculated modulation and thermal smearing contributions of $\sim$10 cm^{-1}. Finally, the top electrode is known to produce a further shift in band position. These shifts have

[1] The observed line positions should be reduced by 8 cm^{-1} to correct for the presence of the superconducting energy gap of the top lead electrode at the temperature of measurement; 1 meV = 8.065 cm^{-1}.

been quantified (17) as a reduction in frequency. In practice these are not significant for adsorbate modes other than the ν(C–H) frequencies from which an estimate (17) of some 30 cm^{-1} can be given when lead is the top electrode. The surface adsorbate can thus be considered as being held in a matrix-isolated condition under the top electrode of the junction.

As we have noted above, almost no pyridine is sufficiently strongly bound to the oxide surface to withstand desorption in high vacuum. In this respect the behavior of the vapor on plasma-grown oxide agrees with the observations of Hansma et al. (8) on untreated air-grown oxide. When the pyridine is trapped on the alumina, by cooling the oxide film, the resulting spectrum closely resembles the fluorided oxide data of Hansma et al. and is substantially different from their heat-treated oxide spectrum.

From examination of our data (Table 1) we suggest the presence of pyridinium species generated by protonation of the pyridine by surface hydroxyl groups acting as Brønsted acid sites. The most convincing evidence in favor of this interpretation is the very broad line at $\sim$2900 cm^{-1} which can only be explained as the ν(N–H) mode, shifted away from its normal position at $\sim$3270 cm^{-1} by a surface oxide anion environment. Possible shifts due to top electrode effects are very much less than this. Such effects can, however, account for the slightly shifted positions of the ν(C–H) modes in the range of $\sim$2960 to $\sim$3100 cm^{-1}. The line at 1250 cm^{-1} may then be attributed to the in-plane $\overset{+}{\text{N}}$–H mode of pyridinium ion. Likewise the out-of-plane $\overset{+}{\text{N}}$–H mode expected at $\sim$900 cm^{-1} is probably being observed at 887 cm^{-1} where it is superimposed on the broad background ν(Al–O) band. The ν(O–H) band of the tunnel barrier shows up in its usual position; it is slightly diminished in strength as compared with the undoped sample, so

relatively few hydroxyls initially present are involved in either Brønsted protonation of pyridine or in weaker hydrogen-bonded interactions. This is consistent with the low doping level achieved. Hydrogen bonding, if present to any notable extent, should be readily detected in the normally band-free 3100- to 3400-cm⁻¹ region of the tunnel spectrum. Since such a band (or bands) is not observed, we conclude that simple hydrogen bond interactions involving OH groups and pyridine are absent.

There is also evidence in our spectra for the formation of coordinately bound pyridine. The lines at 1572 and 1593 cm⁻¹ are both strong and can imply some Lewis acid activity on the oxide surface.

Inspection of the spectrum of Hansma et al. (8) for the fluorided alumina does show a strong band at ∼2900 cm⁻¹ which we argue here is evidence for pyridinium ion. From consideration of lines below 1650 cm⁻¹, they interpreted their results in terms of Lewis acid sites produced by the fluoride pretreatment. We would expect that aqueous fluoride treatment followed by heating to a temperature less than 200°C is likely to leave the surface more than usually hydroxylated (7, 12). Therefore, in addition to the generation of Lewis acid sites, this treatment must at the same time give rise to additional sites of potential Brønsted activity. What is clear is that our procedure of cooling the oxide prior to pumping away excess pyridine vapor gives the same IET spectrum as the fluoriding and heat treatment of Hansma et al.

There is ample evidence from other investigations for Lewis active sites but less for surface hydroxyl as Brønsted sites. For example, Hendra and co-workers (13) have published details of the Raman spectra of pyridine adsorbed on variously treated γ-aluminas and have used, specifically for diagnostic purposes, bands associated with the skeletal motions close to 1000

cm⁻¹ and also the ν(C–H) vibrations. Those found for a heat-treated γ-alumina are listed in Table 1. The bands which remain at very low surface coverages of adsorbed pyridine are footnoted in the table. The 1019-cm⁻¹ band is convincingly demonstrated to be that due to pyridine on a Lewis acid site. At higher coverages additional bands are found; one at 998 cm⁻¹ is attributed to pyridine hydrogen-bonded to surface hydroxyl. However, no bands definitely ascribable to surface pyridinium species were positively characterized even in the more acidic chlorided alumina. The latter was obtained by treatment with carbon tetrachloride while hot under nitrogen.

Recent infrared studies (6) of adsorbed pyridines on γ-alumina and silica-alumina have shown bands (in reciprocal centimeters) at 1618 s, 1580 w, 1495 w, and ∼1450 s for the former and at ∼1620 s, 1547 w, 1495 m, and 1460 s for the latter. In competitive experiments with 2,6-ditertiarybutylpyridine the bands at 1547 and 1495 cm⁻¹ were shown to be due to the pyridinium species, in agreement with earlier work (18). The ∼1450-cm⁻¹ band was assigned to pyridine on Lewis acid surface sites, possibly on electron-deficient oxygen ions rather than surface aluminium cations.

In summary, then, the plasma-grown oxide behaves toward pyridine as does the fluoride-treated air-grown oxide. Both show behavior clearly different from that of the simple heat-treated air-grown oxide in having Lewis acid and Brønsted active sites on which the pyridine is chemisorbed. The pyridine acts as a Lewis base with the former sites and as a proton acceptor with the latter.

CONCLUSION

We conclude that in addition to Lewis acid sites, plasma-grown aluminium oxide, as prepared, does have hydroxyl sites

sufficiently acidic to protonate pyridine, i.e., which are Brønsted active. This is confirmed in its behavior toward phenols (19), benzylamine, and benzylalcohol (20). As to its potential catalytic behavior, we have evidence (20) of its ability to adsorb alkenes by reaction to give chemisorbed alkyl species. Competitive adsorption IETS experiments are now underway to further clarify the question of surface acidity of the plasma-grown material.

REFERENCES

1. Jaklevic, R. C., and Lambe, J., *Phys. Rev. Lett.* 17, 1139 (1966); Lambe, J., and Jaklevic, R. C., *Phys. Rev.* 165, 821 (1968).
2. Keil, R. G., Graham, T. P., and Roenker, K. P., *Appl. Spectrosc.* 30, 1 (1976).
3. Langan, J. D., and Hansma, P. K., *Surface Sci.* 52, 211 (1975).
4. Beck, A. F., Heine, M. A., Caule, E. J., and Pryor, M. J., *Corrosion Sci.* 7, 1 (1967).
5. O'Hanlon, *J. Vac. Sci. Technol.* 7, 332 (1970); Hunt, G. L., and Ritchie, I. M., *J. Chem. Soc. Faraday. Trans. 1*, 68, 1413 (1972).
6. Dewing, J., Monks, G. T., and Youll, B., *J. Catal.* 44, 226 (1976) and references therein.
7. Hughes, T. R., White, H. M., and White, R. J., *J. Catal.* 13, 58 (1969); *J. Phys. Chem.* 71, 2192 (1967).
8. Hansma, P. K., Hickson, D. A., and Schwarz, J. A., *J. Catal.* 48, 237 (1977).
9. McMorris, I. W. N., D. Phil. Thesis, New University of Ulster, Coleraine, Northern Ireland, 1975.
10. Little, L. H., "Infra-red Spectra of Adsorbed Species," p. 233. Academic Press, New York, 1966; Peri, J. B., and Hannan, R. B., *J. Phys. Chem.* 64, 1526 (1960).
11. Katritzky, A. R., and Taylor, P. J., in "Physical Methods in Heterocyclic Chemistry" (Katritzky, A. R., Ed.), Vol. 4, pp. 375 ff. and references therein. Academic Press, New York, 1971.
12. Gill, N. S., Nuttal, R. H., Scaife, P. E., and Sharp, D. W. A., *J. Inorg. Nucl. Chem.* 18, 79 (1961).
13. Hendra, P. J., Turner, I. D. M., Loader, E. J., and Stacey, M., *J. Phys. Chem.* 78, 300 (1974).
14. Kirtley, J., Scalapino, D. J., and Hansma, P. K., *Phys. Rev. B*, 14, 3177 (1976) and references therein.
15. Mulliken, R. S., *J. Chem. Phys.* 23, 1997 (1955).
16. Berezin, V. I., Tatarinov, S. I., Finkel, A. G., and Elkin, M. D., *Opt. Spectrosc.* 40, 385 (1976).
17. Antoniewicz, P. R., *Surface Sci.* 52, 703 (1975); Kirtley, J. R., and Hansma, P. K., *Phys. Rev. B*, 12, 531 (1975).
18. Kiviat, F. E., and Petrakis, L., *J. Phys. Chem.* 77, 1232 (1973).
19. McMorris, I. W. N., Brown, N. M. D., and Walmsley, D. G., *J. Chem. Phys.* 66, 3952 (1977).
20. Brown, N. M. D., and Walmsley, D. G., unpublished results.